Some aspects of the seasonal sea level variations around Spain

J. García-Lafuente,[1] J. Del Río,[1] E. Alvarez Fanjul,[2] D. Gomis,[3] and J. Delgado[1]

[1] Tide gauge stations are used to investigate the seasonal variability of sea level around Spain, which exhibits a well-defined annual cycle and a small but distinguishable semiannual cycle in all stations. The contribution of different sources to observed sea level has been analyzed. The effect of wind and atmospheric pressure has been explored, analyzing sea level residuals computed with a barotropic ocean model forced by the meteorological fields. Sea level corrected for meteorological forcing contains only an annual signal, indicating that the semiannual cycle in the observed sea levels is mainly forced by these meteorological agents. Additional data sets (sea surface temperature satellite images and climatologies) are used to show that the annual cycle is related to the seasonal steric anomaly, which accounts for ~60% of the cycle amplitude. The lack of agreement between the annual phases of sea level and steric anomaly cycles for the stations located in the continental margin of the Atlantic Ocean suggests the existence of other effects in the observed sea levels related to seasonal changes in ocean circulation. On the contrary, open-ocean stations of the Canary Islands have sea level annual cycles phase locked with the steric anomaly cycles, although amplitudes differ significantly from one station to the other. This fact is interpreted as the local response to large-scale seasonal fluctuations of the Canary Current. Sea level cycle in stations within the semienclosed Mediterranean Sea suggests the existence of a hydrological cycle that must include a seasonal barotropic signal through the Strait of Gibraltar.   INDEX TERMS: 4556 Oceanography: Physical: Sea level variations; 4227 Oceanography: General: Diurnal, seasonal, and annual cycles; 3339 Meteorology and Atmospheric Dynamics: Ocean/atmosphere interactions (0312, 4504); 4508 Oceanography: Physical: Coriolis effects; KEYWORDS: sea level, meteorological forcing, steric effect, Mediterranean, Canary Islands, North Atlantic

1. Introduction

[2] Sea level variability at an annual timescale is dominated by the ubiquitous seasonal signal, whose ultimate origin is the annual cycle of solar radiation. The small contribution of gravitational forces of annual and semiannual frequencies present in the tide generating potential [see, e.g., *Pugh*, 1987] is totally negligible in comparison with the much more important meteorological and oceanographic forcing. The most obvious contribution is the thermosteric effect associated with the gain/loss of heat by the upper layer of the ocean, giving rise to the out-of-phase cycle of sea level anomaly in both hemispheres [*Cheney et al.*, 1994; *Tsimplis and Woodworth*, 1994]. Low-frequency variations of air pressure and wind fields associated with the seasonal pattern of atmospheric circulation contribute to the variability of sea level through the inverted barometer response and wind setup, particularly in coastal areas.

However, they also do so by inducing fluctuations in the mean ocean circulation at both regional and global scales [*Wunsch*, 1991]. The net evaporative cycle also contributes to the seasonal sea level signal in the ocean. River runoff can induce large-amplitude seasonal fluctuations of sea level in regions located near river outflows [*Tsimplis and Woodworth*, 1994].

[3] All these contributions are reflected in sea level observations of coastal tide gauges. For low-frequency variability (after removing diurnal, semidiurnal, and higher-frequency tides as well as meteorological fluctuations of a few days period) they can be summarized as

$$y(t) = Z + bt + y_m(t) + y_s(t) + y_o(t) + y_r(t), \qquad (1)$$

where $y(t)$ represents the observed sea level, Z is the mean sea level, the term bt accounts for possible trends, and $y_m(t)$, $y_s(t)$, and $y_o(t)$ are the meteorological, steric, and other contributions, respectively, with more or less regular seasonality. The last term, $y_r(t)$, is the aperiodic contribution that includes interannual variability as well as noise. Terms $y_m(t)$, $y_s(t)$, and $y_o(t)$ may have similar periodicity, in which case they would appear as a unique contribution in the analysis of sea level time series. The first one may be

[1]Departamento de Física Aplicada II, Universidad de Málaga, Málaga, Spain.
[2]Area del Medio Físico, Puertos del Estado, Madrid, Spain.
[3]Institut Mediterrani d'Estudis Avançats, Mallorca, Spain.
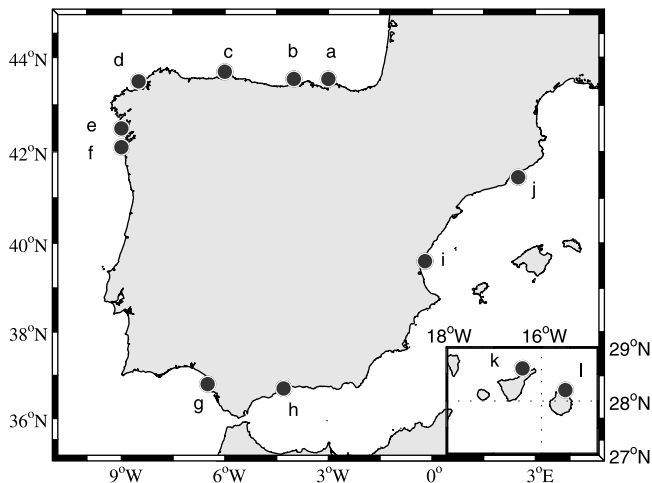
Figure 1. Location of the different stations analyzed in this work: a, Bilbao; b, Santander; c, Gijón; d, La Coruña; e, Villagarcia; f, Vigo; g, Bonanza; h, Málaga; i, Valencia; j, Barcelona; k, Tenerife; and l, Las Palmas. These last two stations are shown in the insert on the bottom right with specific longitude and latitude.

isolated, assuming an inverse barometer response of sea level and some reasonable empirical approach to remove wind setup or by means of more sophisticated methods, such as the output of numerical models in the manner used in this paper. The second term is mainly related to volumetric changes of seawater associated with the seasonal change of heat content in the upper ocean, which could be roughly monitored by means of sea surface temperature (SST). Reasonably, this term is expected to exhibit the purest harmonic behavior taking into account its origin, although advection associated with seasonal changes in the large-scale surface circulation can affect the local steric cycle and disturb the harmonic signal. These changes can also induce sea level slopes via geostrophic balance as well as other local processes (e.g., related to local bathymetry). We have considered these effects together with changes in the barotropic component of the circulation under the third term of equation (1). From a dynamical point of view, this is the most relevant contribution because of its potential to monitor changes in the large-scale circulation at seasonal and longer timescales. An important practical question then arises as to what extent terms $y_s(t)$ and $y_o(t)$ can be isolated from each other. A second question is whether or not term $y_o(t)$ will be distinguishable from the background noise $y_r(t)$. The aim of the present work is the determination of the different terms in equation (1) in different ports around Spain, with special attention paid to term $y_o(t)$.

2. Data

[4] Twelve tide gauge stations located in different ports around Spain and belonging to the Red de Mareografos (REDMAR) network of Puertos del Estado (see Figure 1 for locations) were used to compute monthly mean sea levels from 5 min observations that spanned the period 1992–2001, except for stations c (1996–2001) and e (1997–2001). Historical reanalysis of wind velocity and atmo-

spheric pressure carried out by the Climate Diagnostics Center (CDC), CDC/National Oceanic and Atmospheric Administration/Cooperative Institute for Research in Environmental Science, with a resolution of $2.5° \times 2.5°$ (National Centers for Environmental Prediction (NCEP) data set) were used to obtain monthly time series of these variables at the tide gauge stations. Weekly multiplatform composites of SST images processed by the Intelligent Satellite Data Information System (ISIS), German Aerospatial Center, were used to obtain monthly SST maps and local SST time series by averaging over sea pixels near to the different stations. SST accuracy provided by ISIS is ±0.5 K.

[5] MEDATLAS-2002 [MEDAR Group, 2002] and World Ocean Atlas 2001 [2001] (WOA01) climatologies were used to estimate seasonal dynamic height anomalies (DHA) in the western Mediterranean Sea and eastern North Atlantic, respectively. DHA can be estimated from time series of conductivity-temperature-depth (CTD) casts, which include salinity effects, as by Tsimplis and Rixen [2002], or from reliable net heat fluxes but neglecting salinity, as by Efthymiadis et al. [2002]. The approach followed here is to compute an average DHA seasonal cycle from the climatologies mentioned in section 2 over a domain that includes the eastern part of the North Atlantic Ocean and the Western Mediterranean Sea. The reason for using climatologies instead of time series is that historical data have important spatial and/or temporal lags during the decade spanned by the observations, which clearly restricts the utility of the computed series of DHA.

[6] Meteorological sea level residuals at the different ports were generated within the European Union project Hindcast of Dynamic Processes of the Ocean and Coastal Areas of Europe (HIPOCAS) [Guedes Soares et al., 2002]. The model downscales the historical reanalysis made by CDC by means of the atmospheric Regional European Model (REMO). Atmospheric sea level pressure obtained by this method matches quite well the observations ($r > 0.96$; root-mean-square error (RMSE) between 1.15 and 2.16 mb). Differences between hindcast and measured winds are larger. A higher correlation ($r \sim 0.85-0.9$; RMSE $\sim 2 \text{ m s}^{-1}$) is found at the Bay of Biscay. The correlation diminishes in the neighborhood of the Strait of Gibraltar, where local effects are important ($r \sim 0.5-0.65$; RMSE $\sim 3.0 \text{ m s}^{-1}$) and the resolution of the downscaled atmospheric model is still clearly insufficient for the wind field. In a second stage the model uses the new high-resolution wind and pressure fields to generate a 44 year data set of waves and sea level residuals. In the Mediterranean Sea, residuals were computed by means of a barotropic version of the Hamburg Shelf Circulation Model (HAMSOM) [Alvarez Fanjul et al., 1997] over the domain $30°-47°$N and $-12°-35°$E, which includes the Mediterranean Sea and the eastern sector of the North Atlantic Ocean. This version of the code is routinely operated by Puertos del Estado as part of the Nivmar sea level forecast application [Alvarez Fanjul et al., 2001]. The comparison of HAMSOM computed and REDMAR observed residuals is very satisfactory ($r \sim 0.87-0.82$; RMSE $\sim 5.2-6.4$ cm), particularly for low frequencies. On the other hand, the Canary Islands region is too close to the boundary domain to compute reliable
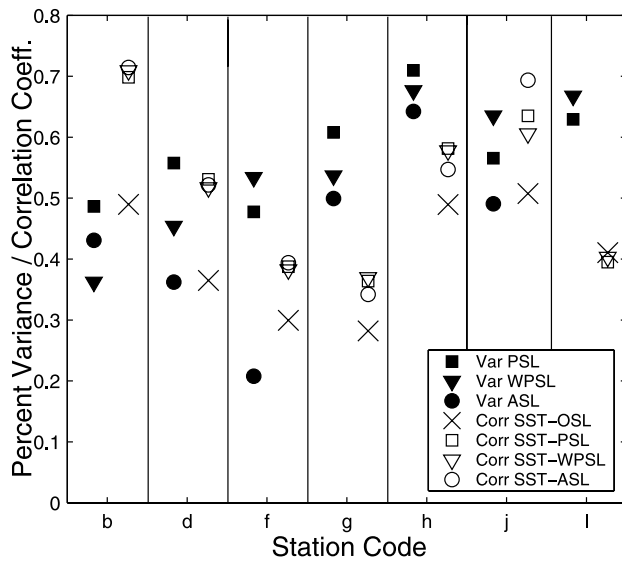
Figure 2. Percentage of variance that remains after removing the meteorological contribution from observed sea level (OSL). Solid squares indicate the remaining variance after barometrically correcting the OSL (PSL label), solid triangles are for a correction that combines inverted barometric response plus empirical wind setup (WPSL label), and solid circles are for HAMSOM residuals (ASL label). Station l does not have the ASL symbol because HAMSOM residuals cannot be computed there (see text for details). Open symbols are for correlation between SST and the sea level series obtained after removing the meteorological contribution with different methods. The labels on the x axis are the station codes (Figure 1). For clarity, some stations are not included as they are close to other stations which behave similarly (stations a and c are well represented by station b, for instance).

HIPOCAS/HAMSOM residuals. Except for stations k and l within this region, the residuals from HIPOCAS/HAMSOM are used in this paper to remove the meteorological forcing in the observed sea level.

3. Results

3.1. Meteorological Influence, $y_m(t)$

[7] Meteorological forcing influences sea level through two different mechanisms. The first one is the inverted barometer response and wind setup, which is analyzed in this section. The second one is by inducing fluctuations of the large-scale ocean circulation, whose signatures in coastal sea level, if any, fall into category $y_o(t)$ of equation (1) and are discussed in section 3.3.

[8] Three methods have been used to isolate the first type of meteorological influence from observed sea level (OSL): inverted barometer; inverted barometer plus empirical wind setup of the form $\xi = -Cv$, v being the wind component that yields maximum sea level gain at each station (usually the along-shore, wind-inducing upwelling) and C being a regression constant that can be interpreted as the frequency-averaged sea level gain, which in turn could be related to the shelf width and to the Coriolis parameter, as by

Sandstrom [1980]; and a third method that uses the residuals computed by the HAMSOM model. Figure 2 shows that any of the methods reduces the monthly mean sea level variance of the original OSL significantly. The atmospheric pressure, which accounts for 30–50% of the variance, is the main agent explaining this reduction. Theoretically, the latter procedure is the best to remove meteorologically induced signals because the response of sea level is computed directly from the equations of motion instead of assuming an empirical wind setup correction and an inverted barometer response, which is questionable in semienclosed seas such as the Mediterranean [*Garrett*, 1983; *Candela et al.*, 1989; *Le Traon and Gauzelin*, 1997]. In practice, this method also performs better than the others (Figure 2), reducing the OSL
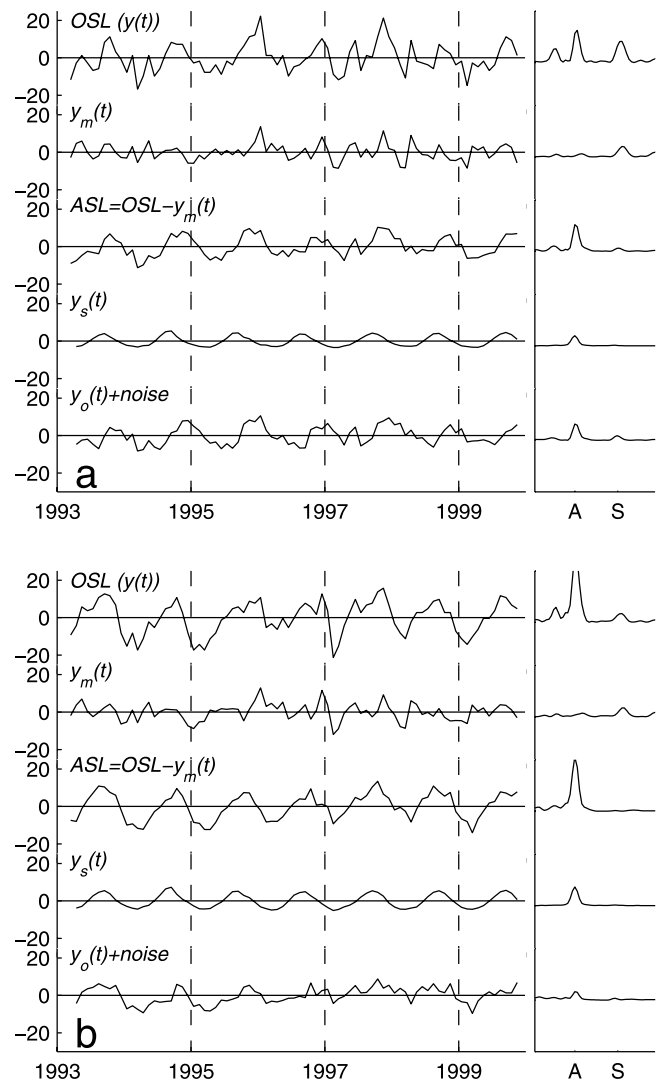
Figure 3. Plots of the different contributions of sea level and associated spectra for (a) Santander (station b) and (b) Valencia (station i). Annual (A) and semiannual (S) frequencies have been marked in spectrum plots. From top to bottom the plotted series are observed sea level (label OSL), meteorological residual (label $y_m(t)$), sea level corrected for meteorological influence (label ASL), steric contribution (label $y_s(t)$), and other effects plus noise (label $y_o(t)$ + noise).

Table 1. Parameters of the Fitting of Model (2) to Different Time Series in All Stations

Station	OSL[a]				ASL[b]				SST[c]		ASL-SST[d]	
	A_a, cm	φ_a, deg	A_s, cm	φ_s, deg	A_a, cm	φ_a, deg	A_s, cm	φ_s, deg	A_a, °C	φ_a, deg	c	Lag
a	5.5 ± 2.2	293 ± 23	3.0 ± 2.0	257 ± 39	5.5 ± 1.1	304 ± 11	1.1 ± 0.9	282 ± 49	4.5 ± 0.2	220 ± 2	0.75	−2.5
b	6.0 ± 2.3	300 ± 23	3.0 ± 2.1	256 ± 40	6.0 ± 1.1	310 ± 11	1.1 ± 0.9	278 ± 48	4.5 ± 0.2	220 ± 2	0.79	−2.5
c	6.0 ± 3.4	318 ± 33	3.5 ± 2.9	282 ± 47	4.9 ± 1.4	318 ± 16	1.4 ± 1.3	298 ± 52	3.7 ± 0.2	224 ± 3	0.51	−2.5
d	4.6 ± 2.8	317 ± 36	3.4 ± 2.3	262 ± 38	4.2 ± 1.5	321 ± 21	1.3 ± 1.4	293 ± 62	2.4 ± 0.2	228 ± 4	0.58	−2.5
e	5.1 ± 4.8	344 ± 54	3.1 ± 4.2	264 ± 76	3.6 ± 2.5	332 ± 41	0.9 ± 2.6	300 ± 163	1.9 ± 0.3	225 ± 4	0.24	−2.5
f	3.8 ± 3.1	329 ± 48	3.5 ± 2.5	275 ± 41	2.9 ± 1.4	306 ± 27	1.2 ± 1.4	310 ± 61	1.9 ± 0.3	225 ± 4	0.44	−2.5
g	3.8 ± 2.4	252 ± 37	2.1 ± 2.2	261 ± 60	3.3 ± 1.7	292 ± 31	1.0 ± 1.6	288 ± 96	3.3 ± 0.2	220 ± 3	0.37	−2.5
h	5.7 ± 1.6	264 ± 16	0.9 ± 1.6	273 ± 41	5.3 ± 1.3	288 ± 14	0.7 ± 1.3	18 ± 113	3.5 ± 0.2	216 ± 3	0.61	−2.5
i	9.5 ± 2.2	246 ± 13	2.6 ± 2.0	253 ± 44	8.4 ± 1.2	256 ± 8	0.8 ± 1.2	255 ± 87	6.2 ± 0.3	218 ± 2	0.75	−0.5
j	7.0 ± 1.8	260 ± 15	2.9 ± 1.9	261 ± 35	6.6 ± 0.8	274 ± 7	1.4 ± 0.9	280 ± 33	6.2 ± 0.3	219 ± 2	0.77	−1.5
k	7.6 ± 1.6	237 ± 13	1.6 ± 1.5	192 ± 54	6.5 ± 1.3	246 ± 11	0.8 ± 1.1	173 ± 85	2.1 ± 0.3	250 ± 3	0.51	0
l	4.5 ± 1.5	239 ± 20	1.7 ± 1.6	208 ± 51	3.3 ± 1.1	258 ± 18	0.8 ± 1.3	217 ± 90	1.9 ± 0.2	257 ± 4	0.45	0

[a]Amplitude and phase (and their 95% confidence limits) of annual (subindex a) and semiannual (subindex s) cycles of the observed sea levels.
[b]Same results for the meteorologically corrected sea levels.
[c]Amplitude and phase of the annual cycle of sea surface temperature.
[d]Correlation coefficients between ASL and SST series and the lag (months) between them; a negative sign indicates delay of ASL.

variance to 50% on average and as much as 70–80% in some ports of northern Spain. As a rule, the more to the north the station is, the greater the variance reduction, a fact mentioned by *Pugh* [1987] and related to stormier weather in higher latitudes. Residuals hindcast by HAMSOM are identified with the term $y_m(t)$ in equation (1). The difference between OSL and this prediction will be called adjusted sea level (ASL) and would only include contributions $y_s(t)$, $y_o(t)$, and noise of equation (1).

[9] The central panels of Figures 3a and 3b show two examples of ASL series in stations b and i. The attached spectra show that the semiannual signal in OSLs is almost totally removed in ASLs, which clearly indicates a meteorological origin of the semiannual cycle in OSLs. The annual cycle in ASLs is hardly modified and becomes more regular, suggesting a different source for it, presumably the steric effect. This reasoning is supported by the increase, on average, of the correlation coefficient between ASL and SST with respect to that obtained for OSL and SST (Figure 2).

[10] Because the spectral analyses of sea level series show a clear dominance of annual and (to a lesser extent) semiannual signals, with a minor contribution of interannual variability (see inserts in Figures 3a–3b), it seems justified to use the harmonic model

$$y(t) = Z + bt + A_a \cos(w_a t - \varphi_a) + A_s \cos(w_s t - \varphi_s) \quad (2)$$

to analyze these signals. In equation (2), A_a, φ_a, and w_a (A_s, φ_s, and w_s) are the amplitude, phase, and frequency of the annual (semiannual) signal, respectively, Z is the mean sea level, and b is the sea level trend. The latter is below the 95% confidence level in all peninsular stations, but it is 2.4 ± 1.2 and 1.9 ± 1.1 mm yr^{-1} at stations k and l in the Canary Islands, respectively. These values are in the upper limit of 1–2 mm yr^{-1} interval usually taken as reference in studies of long-term sea level trends [*Douglas*, 2000], an agreement that may be coincidental as a 10 year period is not enough to compute long-term trends (part of this trend is probably related to interdecadal variability such as the North Atlantic Oscillation). These values are not far from the global sea level trend of 3 mm yr^{-1} computed from altimetric

data spanning a similar period as the tide gauge data of this work [*Nerem*, 1999].

[11] The result of fitting equation (2) to OSLs and ASLs is presented in Table 1. As expected, annual amplitudes dominate the OSL, the greatest ones being found inside the Mediterranean Sea, far from the Strait of Gibraltar (stations i and j) and in station k in the Canary Islands. Semiannual signals in ASL fall below the 95% confidence interval and become irrelevant, while annual signals are only slightly modified with regard to OSL series. The annual signal of ASLs in northern Spain ports of the Atlantic Ocean has phase over 300° (seasonal peak in November) and decreases to ~270° (end of September, beginning of October) in the Mediterranean Sea. The Canary Island region reaches the maximum earlier (~250° or beginning of September).

3.2. Steric Contribution, $y_s(t)$

[12] Steric contribution is obviously related to SST. Table 1 gives the amplitude and phase of the SST annual cycle from equation (2) (semiannual cycle is totally negligible) in the neighborhood of the different ports. The signal has greater amplitude in the Mediterranean Sea, far from the Strait of Gibraltar, and lower amplitude in stations k and l (Canary Islands) and e and f (Galicia). The low amplitude in the Canary Islands is attributed to the smooth contrast between summer and winter air temperatures, while the reduced annual cycle off Galicia would be related to the upwelling season, as discussed in section 3.3. Table 1 also shows the correlation between ASL and SST and the lag for which the correlation peaks. ASL delays SST in all ports of the Iberian Peninsula by weeks to months, the delay being more noticeable in the Atlantic ports than in the Mediterranean Sea. Both series are simultaneous (within the 95% confidence interval) in the Canary Islands region.

[13] The scatterplot of Figure 4 shows a reasonably good linear dependence between ASL and SST annual amplitudes, except for stations k and g, which are outside the 95% confidence interval of the regression line. The anomalous high-amplitude response for a reduced SST signal in at station k is probably related to seasonal changes in the ocean circulation, which would be included in term $y_o(t)$ of equation (1), while the poor response at station g, placed nearby the Guadalquivir River mouth, is likely related to the
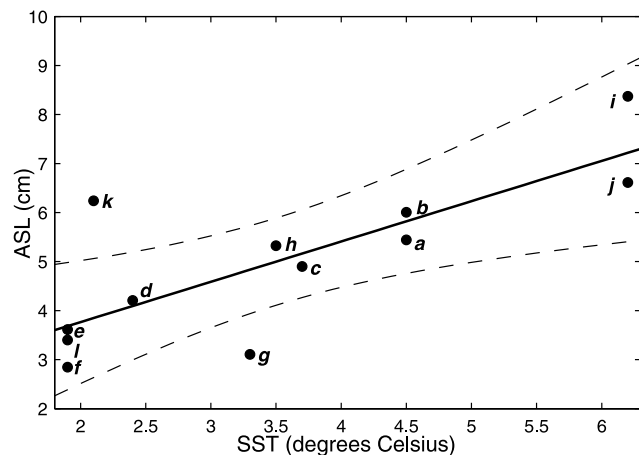
Figure 4. Scatterplot of SST-ASL amplitudes of annual cycles. The straight line is the linear fit, and dashed lines are the 95% confidence interval. Labels beside each point refer to the station (see Figure 1).

river discharge, which has a seasonal cycle opposite to that of the thermal expansion of seawater.

[14] The regular annual cycle of ASLs (Figures 3a–3b) and the reasonably good agreement of ASL and SST amplitudes shown in Figure 4 reveal the importance of the steric sea level cycle on ASL. However, phases of ASL and SST do not agree so well (Table 1). The steric cycle is dominated by the thermal expansion of seawater, salinity changes playing a minor role. SST is only an indirect indicator of the steric anomaly in the sense that thermal expansion relates to the heat content of seawater rather than to the surface temperature. The decrease of SST after its seasonal peak is not necessarily echoed by the heat content of the water column, which could go on increasing during weeks or even months.

[15] The DHA, directly related to the thermal expansion of seawater, is a more reliable indicator of the heat content. It is used next to investigate this delay. Figure 5a shows maps of amplitude and phase of the DHA annual cycle in the Atlantic Ocean obtained from WOA01 using 500 m as the reference depth, a level deep enough to be insensitive to surface energy inputs. Figure 5b is for the Mediterranean Sea, using the MEDATLAS database and the same reference depth. Amplitude contours reproduce the main features of the spatial distribution of ASL such as the increase of amplitude toward the east along the northern Spanish coast, the amplitude reduction on the western facade of the Galician coast (ports e and f), the marked difference of amplitude between Canary Islands ports k and l, and the noticeable increase of amplitude toward the interior of the Mediterranean Sea. However, Table 2 indicates that DHA amplitudes are, on average, 60% of those of ASL, and phases are usually smaller (DHA peaks earlier), although stations k and l (Canary Islands) are important exceptions. More important, phases of DHA are ∼30° greater than phases of SST in all peninsular ports (Table 2), a difference that provides an estimation of the delay mentioned above. Again, stations in the Canary Islands are exceptions to this rule: It is noteworthy that ASL, SST, and DHA phases

coincide (within the 95% confidence interval) in this region, suggesting that the lack of phase agreement in the peninsular ports is a consequence of continental shelf response.

[16] On the basis of these results, an estimation of term $y_s(t)$ in equation (1) has been made by means of a linear regression of the form $y_s(t) = a \cdot \text{SST}(t - \tau)$ using the SST series as input, with the coefficient a given by the linear fit in Figure 4 and with the time lag τ equal to the phase difference between DHA and SST, in order to account for the delay between both series (therefore phases of $y_s(t)$ and DHA are identical). By doing this, we attempt to isolate the purely steric part of the ASL from other sloping effects related to changes in the (baroclinic) large-scale circulation, which may also contribute to the seasonal signal of the OSL under term $y_o(t)$. An example of a $y_s(t)$ time series at stations b and i is shown in panel $y_s(t)$ of Figures 3a and 3b.

3.3. Other Seasonal Effects, $y_o(t)$

[17] The bottom panel of Figures 3a–3b is the difference between ASL and $y_s(t)$ at stations b and i, which would represent term $y_o(t)$ plus noise in equation (1). In general, it exhibits distinguishable annual variability, from which the annual cycle presented in Table 2 has been estimated. This variability is tentatively related to seasonal changes of the large-scale ocean circulation and is analyzed in sections 3.3.1–3.3.4.

3.3.1. Amplitude Difference Between Canary Island Ports

[18] ASL amplitude at station k is twice the amplitude at station l, despite the fact that the SST signal in the former is only 10% greater than in the latter (Table 1). This discrepancy was already referred to by *Tsimplis and Woodworth* [1994] (see http://www.nbi.ac.uk/psmsl/datainfo/seasonal. msl.tables) and reflects an actual feature that is confirmed by the sharp amplitude gradient between stations k and l in the map of Figure 5a. Judging from results in Figure 4 and Table 2, it is Tenerife (k) that presents anomalously high ASL amplitude with respect to the value that would be expected from the seasonal steric cycle. Station l, on the contrary, has an ASL cycle that agrees quite well with its steric cycle. Actually, Table 2 shows that this station hardly needs the existence of an ASL − $y_s(t)$ residual cycle (term $y_o(t)$ in equation (1)) to explain the ASL cycle, while station k does.

[19] Figure 5a depicts a large eddy-like structure northwest of the Canary Islands which would have anticyclonic (cyclonic) circulation associated in summer/autumn (winter/spring). When superposed onto the mean flow, it would reproduce the seasonal variation in the Canary Current reported by *Navarro-Pérez and Barton* [2001], who indicate a reinforcement (weakening) of the southward flow between Tenerife and the African coast in summer (winter) and a southward signal of the flow west of Tenerife in winter but a northward tendency in summer. This overall scenario of stronger equatorward flow closer to the coast in summer and further offshore in winter also agrees with the results of *Stramma and Siedler* [1988], and it would be related to the seasonal upwelling cycle in the region and to the position of the subtropical gyre. Hence the large ASL amplitude obtained
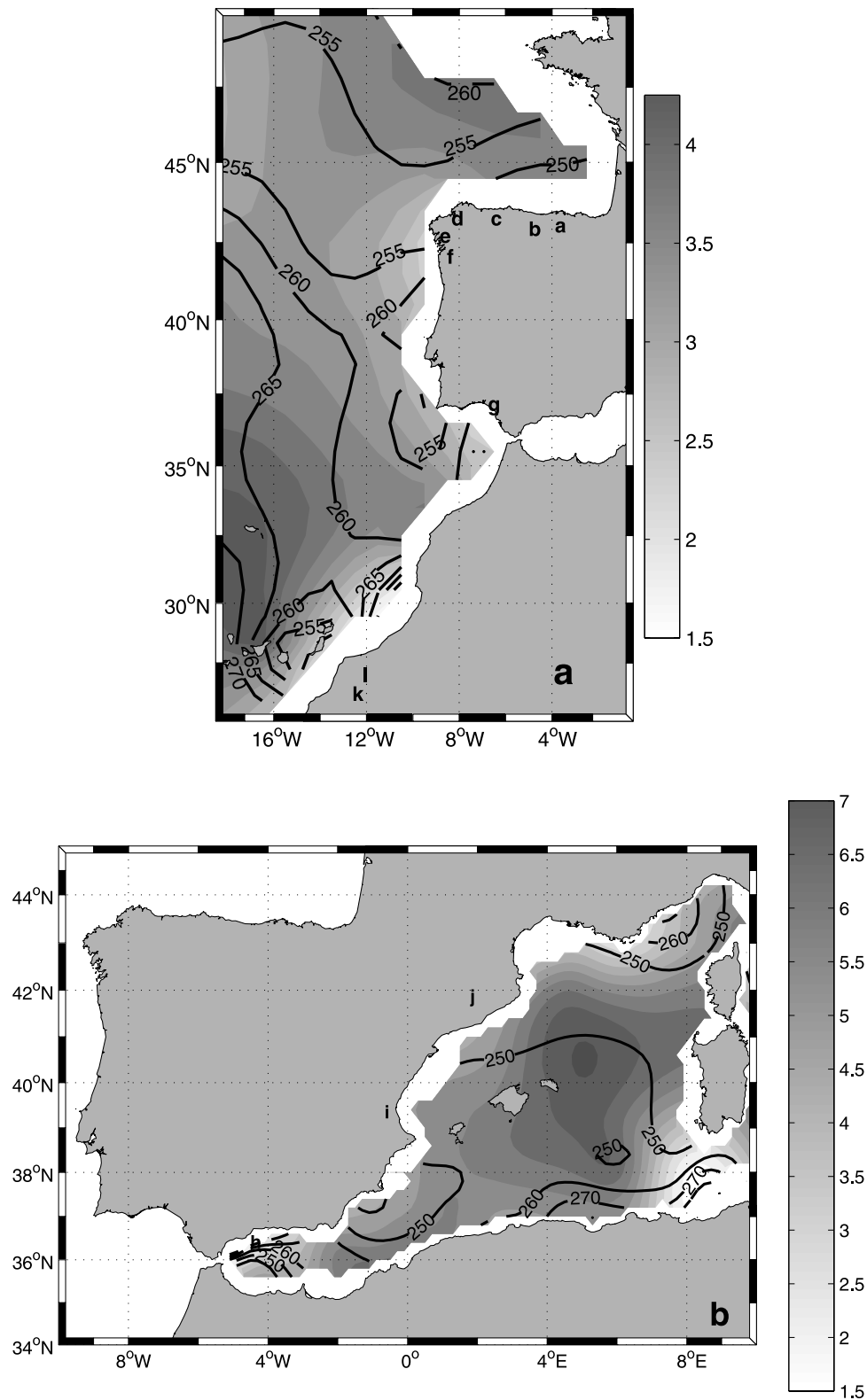
Figure 5. (a) Contours of amplitude and phase of the steric height anomaly annual cycle in the North Atlantic computed from WOA01 climatology. (b) Same as Figure 5a, but for the Mediterranean Sea, computed from the MEDATLAS 2002 climatology. Letters are station codes.

Table 2. Amplitude and Phase of the Annual Cycle of the Dynamic Height Anomaly (Block DHA) Near Some Selected Tide Gauge Stations[a]

Station	DHA		ASL[b]		A_{dha}/A_{asl}[c]	$y_o(t) \approx ASL - y_s(t)$[d]	
	A_a	φ_a	A_a	φ_a		A_a	φ_a
a	3.6 ± 0.9	250 ± 15	5.5 ± 1.1	304 ± 11	0.65	4.5 ± 2.1	344 ± 26
b	3.6 ± 0.9	250 ± 15	6.0 ± 1.1	310 ± 11	0.60	5.2 ± 2.2	346 ± 22
c	3.4 ± 0.9	250 ± 15	4.9 ± 1.4	318 ± 16	0.69	4.7 ± 2.3	354 ± 27
d	2.5 ± 1.2	250 ± 25	4.2 ± 1.5	321 ± 21	0.59	4.0 ± 2.7	348 ± 38
e	1.9 ± 1.2	255 ± 25	3.6 ± 2.5	332 ± 41	0.53	. . .	. . .
f	1.9 ± 1.2	255 ± 25	2.9 ± 1.4	306 ± 27	0.65	. . .	. . .
g	2.2 ± 1.3	270 ± 20	3.3 ± 1.7	292 ± 31	0.67	. . .	. . .
h	2.1 ± 1.2	270 ± 20	5.3 ± 1.3	288 ± 14	0.40	2.8 ± 2.5	306 ± 52
i	4.9 ± 0.9	255 ± 10	8.4 ± 1.2	256 ± 8	0.58	3.4 ± 1.8	257 ± 33
j	4.6 ± 0.9	240 ± 10	6.6 ± 0.8	274 ± 7	0.70	3.7 ± 1.6	322 ± 24
k	4.1 ± 0.8	260 ± 10	6.5 ± 1.3	246 ± 11	0.63	4.9 ± 2.3	241 ± 27
l	2.9 ± 0.8	250 ± 10	3.3 ± 1.1	258 ± 18	0.88	1.7 ± 1.6	260 ± 53

[a]A spatially averaged amplitude and phase error has been assigned to each estimation. Notice that DHA phases coincide with phases of $y_s(t)$ (see text).
[b]In italics, repetition of the information shown in Table 1 to facilitate comparison.
[c]Ratio of amplitudes of ASL and DHA.
[d]Difference between the annual cycles of ASL and $y_s(t)$, which could be interpreted as an estimation of term $y_o(t)$ in equation (1). Empty cells indicate an amplitude less than its computed error and therefore no significant cycle.

at station k could be the result of this large-scale seasonal fluctuation of the Canary Current.

3.3.2. Phase Delay in Northern Spain

[20] Table 2 shows a systematic phase delay of ~ 2 months ($60°$) between ASL and $y_s(t)$ in the ports of northern Spain, which largely accounts for the dominant $y_o(t) \approx ASL - y_s(t)$ cycle of these stations. This phase mismatch is harder to explain. As mentioned by *Pugh* [1987], phases of the annual cycle estimated from observed sea level have a clear tendency to increase toward the north in the Northern Hemisphere, maxima being reached as late as December or even January in the far north. In the Biscay Bay the hydrological cycle and the strong river runoffs could explain this delay, but seasonal changes in the surface circulation are likely candidates too. *Pingree and Le Cann* [1990] mention an eastward surface flow of warm and saline water along the shelf of northern Spain during winter, the flow being a prolongation of the Poleward Current coming from the western Iberian shelf. This surface flow may be enhanced by the dominant westerlies during this season [*Frouin et al.*, 1990]. On the contrary, the more frequent easterlies in spring/summer could generate upwelling and westward wind-driven currents that hamper the entrance of the Poleward Current. Some hints for the seasonal variability of shelf currents along northern Spain are provided by *Lavin et al.* [1998] and *Gil et al.* [2002]. Geostrophic adjustment of the shelf currents would induce an additional sea level cycle of the right sign to shift the overall seasonal maximum toward winter months. Obviously, this speculative reasoning needs further research.

3.3.3. Reduced Amplitude Off Galician Coast

[21] In contrast with the stations in the northern coast, stations e and f in the western facade of the Galician coast do not need any additional $y_o(t)$ term to explain the seasonal variability (Table 2). This result deserves some comment. Figure 2 shows that term $y_m(t)$ in equation (1) accounts for $\sim 80\%$ of the observed seasonal variance in these stations, suggesting a strong response to meteorological forcing, particularly to winds (compare filled square and circle symbols in column f of Figure 2). As a consequence, these ports have a reduced ASL cycle (Table 1). On the other hand, the Galician coast is part of the upwelling system related to the North Atlantic subtropical gyre, a system that undertakes seasonal variability in response to seasonal winds. The upwelling cycle peaks in summer [*Wooster et al.*, 1976], which in turn causes a seasonal SST cycle opposite to that of thermal heating that reduces the amplitude of the total SST cycle (Table 1). This feature, which is also well captured in the spatial distribution of the DHA amplitude of Figure 5a, implies a small $y_s(t)$ cycle in agreement with the ASL cycle. Within the 95% confidence interval, both signals cancel each other, and the term $y_o(t)$ is not needed to explain the residual.

3.3.4. Sea Level and Water Mass Balance Within the Mediterranean Sea

[22] The residual $y_o(t)$ cycle in the Mediterranean Sea ports could be related to a seasonal barotropic transport through the Strait of Gibraltar. The semienclosed nature of this sea facilitates the formulation of a water balance equation, which helps justify the hypothesis. There are three different sources contributing to the seasonal ASL signal at basin scale: the steric effect (ST), which only affects volumetric changes but not mass imbalance, fresh water flux associated with the net evaporative cycle (FW), and the above-mentioned possible seasonal signal in the net flow through the strait (FG), the last two affecting the water mass content. They should verify an equation of the form

$$ASL = ST + FW + FG + noise, \qquad (3)$$

where ASL is the representative monthly mean sea level of the basin. At local scale, seasonal changes in the surface circulation in the vicinity of strong currents (such as the Alboran Basin) may have noticeable influence on the ASL nearby. *Bouzinac et al.* [2003] show that the first empirical orthogonal function computed from altimetric data, which mainly accounts for the seasonal cycle, exhibits sharp spatial gradients in the amplitude distribution depicting the Alboran gyres, while amplitude variations are smoother in the remainder of the western Mediterranean basin. Figure 5b agrees with this description. If so, station h, under the influence of the gyres, is less representative of the basin, but stations i and j, far from the Strait, would be.

[23] The freshwater flux in the Mediterranean Sea has recently been recalculated from European Centre for Medium-Range Weather Forecasts data by *Boukthir and Barnier* [2000]. They provide figures of the monthly freshwater deficit, from which an annual cycle of 2.2 ± 0.2 cm month^{-1} with a maximum deficit in September–October ($278° \pm 5°$) is readily determined. NCEP reanalysis [*Mariotti et al.*, 2002] gives a similar hydrological cycle, with a slightly smaller amplitude and a deficit peak shifted toward early September. Time integration of the freshwater flux leads to an associated seasonal sea level signal of 4 ± 0.4 cm amplitude, peaking in late June ($172° \pm 5°$). If the ST component is assumed to be well represented by DHA at basin scale and taking a representative cycle of 5 ± 1 cm and $250° \pm 10°$ for DHA from Figure 5b, which agrees with the values reported by *Bouzinac et al.* [2003], then ST + FW in equation (3) is 7.1 ± 1.8 cm at $216° \pm 14°$. While ASL amplitudes at stations i and j fall within the error interval of this sum, phases are clearly outside this interval (see Table 1), even when doubling the uncertainties in ST and FW (sum = 7.1 ± 3.5 cm, $216° \pm 29°$). Term FG in equation (3) must be significantly different from zero or, in other words, a seasonal cycle in the net flow through the Strait of Gibraltar would be needed to explain the seasonal sea level cycle of the Mediterranean Sea. An estimation of FG can be made from equation (3). A representative value of ASL is difficult to determine, particularly because of the phase difference of ASL between stations i and j. As a rough guess, we take 7.0 ± 1.5 cm and $270° \pm 15°$ for amplitude and phase, which cover the values of these stations in Table 1 and also most of the range of the values reported by *Tsimplis and Woodworth* [1994] for coastal stations over the western Mediterranean Sea. This in turns implies a seasonal net flow cycle of 0.032 ± 0.020 Sv (for a Mediterranean area of 2.5×10^{12} m^2) with maximum value at $244° \pm 35°$ (August–September), which does not disagree with the seasonal cycle of 0.077 ± 0.044 Sv, $234° \pm 33°$ computed by *García Lafuente et al.* [2002] from an almost 3-year-long time series of current meter observations in the Strait of Gibraltar.

4. Conclusions

[24] Annual cycles computed from the sea level data set analyzed in this study fit well within the global pattern depicted in worldwide studies of seasonal signal, like the work by *Tsimplis and Woodworth* [1994]. Three different contributions to the OSL related to different driving forces have been considered. The first one is the low-frequency meteorological variability that introduces a semiannual signal in the OSL, which has been isolated using the output of a suitable numerical model. This contribution (term $y_m(t)$ in equation (1)) was then subtracted from the OSL to obtain the so-called ASL. Semiannual signals in ASL are almost totally removed, while annual signals are hardly modified by this correction, suggesting that the steric effect, mainly thermal expansion, is the likely main source for it. Therefore a high correlation between SST and ASL is expected, though it is not always obtained (Table 1). The rather regular annual oscillation of ASL (Figures 3a–3b) and SST (not shown) suggests the use of the harmonic model equation (2) to study the seasonal signal. Amplitudes of

ASL and SST are well correlated (Figure 4), but phases do not agree with the exception of the open-ocean stations of the Canary Islands. The good relationship of amplitudes was used to make an estimation of a steric cycle ($y_s(t)$) by means of a linear model. Climatological data were used to make an estimation of the phase lag between SST and DHA cycles based on the hypothesis that this lag represents the delay between maximum SST and maximum heat contained in the water column. This lag was introduced in the linear model to compute $y_s(t)$, which therefore has the same phase as DHA. When the steric contribution so computed is extracted from the ASL series, it still remains a residual, with annual periodicity in most stations.

[25] Some speculative reasons have been put forward in order to explain this residual term, identified with term $y_o(t)$ plus noise in equation (1). The great residual in station k (Tenerife port) could be the consequence of a geostrophic adjustment to seasonal changes in the Canary Current. The absence of a significant residual cycle off the Galician coast would be associated with the upwelling seasonal cycle. It is probable that the observed annual cycle of ASL in the Mediterranean Sea needs the existence of a seasonal signal in the net barotropic flow through the Strait of Gibraltar in addition to the mean net flow to compensate evaporative losses in the basin. This contribution would appear under term $y_o(t)$ along with the freshwater cycle. The spatially coherent phase delay in the ports of northern Spain with reference to climatological steric anomalies could be connected with seasonal variations of the surface layer circulation in the continental shelf. In summary, important features of the ocean circulation would be captured by tide gauge stations measuring sea level. These measurements can therefore be considered as suitable and cost effective indices to detect interannual variability of those features.

References

Alvarez Fanjul, E., B. Pérez Gómez, and I. Rodríguez Sanchez-Arévalo (1997), A description of the tides in the eastern North Atlantic, *Prog. Oceanogr.*, *40*, 217–244.

Alvarez Fanjul, E., B. Pérez, and I. Rodríguez (2001), NIVMAR: A storm-surge forecasting system for Spanish waters, *Sci. Mar.*, *60*, 145–154.

Boukthir, M., and B. Barnier (2000), Seasonal and inter-annual variations in the surface fresh water flux in the Mediterranean Sea from the ECMWF re-analysis project, *J. Mar. Syst.*, *24*, 343–354.

Bouzinac, C., J. Font, and J. Johannessen (2003), Annual cycles of sea level and sea surface temperature in the western Mediterranean Sea, *J. Geophys. Res.*, *108*(C3), 3059, doi:10.1029/2002JC001365.

Candela, J., C. D. Winant, and H. L. Bryden (1989), Meteorologically forced subinertial flows through the Strait of Gibraltar, *J. Geophys. Res.*, *94*, 12,667–12,679.

Cheney, R., L. Miller, R. Agreen, N. Doyle, and J. Lillibridge (1994), TOPEX/POSEIDON: The 2-cm solution, *J. Geophys. Res.*, *99*, 24,555–24,564.

Douglas, B. C. (2000), Sea level change in the era of the recording tide gauge, in *Sea Level Rise: History and Consequences*, edited by B. C. Douglas, M. S. Kearney, and S. P. Leatherman, pp. 37–64, Academic, San Diego, Calif.

Efthymiadis, D., F. Hernandez, and P. Y. Le Traon (2002), Large-scale sea level variations and associated atmospheric forcing in the subtrop-

ical north-east Atlantic Ocean, *Deep Sea Res., Part II*, *49*, 3957–3981.

Frouin, R., A. F. G. Fiuza, I. Ambar, and T. J. Boyd (1990), Observations of a poleward surface current off the coasts of Portugal and Spain during winter, *J. Geophys. Res.*, *95*, 679–691.

García Lafuente, J., J. Delgado, J. M. Vargas, M. Vargas, F. Plaza, and T. Sarhan (2002), Low-frequency variability of the exchanged flows through the Strait of Gibraltar during CANIGO, *Deep Sea Res., Part II*, *49*, 4051–4067.

Garrett, C. (1983), Variable sea level and strait flows in the Mediterranean: A theoretical study of the response to meteorological forcing, *Oceanol. Acta*, *6*, 79–87.

Gil, J., L. Valdés, M. Moral, R. Sánchez, and C. García Soto (2002), Mesoscale variability in a high-resolution grid in the Cantabrian Sea (southern Bay of Biscay), May 1995, *Deep Sea Res., Part I*, *49*, 1591–1607.

Guedes Soares, C., J. C. Carretero Albiach, R. Weisse, and E. Alvarez Fanjul (2002), A 40 years hindcast of wind, sea level and waves in European waters, paper presented at the 21st International Conference on Offshore Mechanics and Arctic Engineering, Am. Soc. of Mech. Eng., Olso.

Lavin, A., L. Valdés, J. Gil, and M. Moral (1998), Seasonal and inter-annual variability in properties of surface water off Santander, Bay of Biscay, 1991–1995, *Oceanol. Acta*, *21*, 179–190.

Le Traon, P. Y., and P. Gauzelin (1997), Response of the Mediterranean mean sea level to atmospheric pressure forcing, *J. Geophys. Res.*, *102*, 973–984.

Mariotti, A., M. V. Struglia, N. Zeng, and K. M. Lau (2002), The hydrological cycle in the Mediterranean region and implications for the water budget of the Mediterranean Sea, *J. Clim.*, *15*, 1674–1690.

MEDAR Group (2002), MEDATLAS/2002 database: Mediterranean and Black Sea database of temperature salinity and bio-chemical parameters, in *Climatological Atlas* [CD-ROM], Fr. Res. Inst. for Exploit. of the Sea, Issy-les-Moulineaux, France.

Navarro-Pérez, E., and E. D. Barton (2001), Seasonal and interannual variability of the Canary Current, *Sci. Mar.*, *65*, 205–213.

Nerem, R. S. (1999), Measuring very low frequency sea level variations using satellite altimetric data, *Global Planet. Change*, *20*, 157–171.

Pingree, R. D., and B. Le Cann (1990), Structure, strength and seasonality of the slope currents in the Bay of Biscay region, *J. Mar. Biol. Assoc.*, *70*, 857–885.

Pugh, D. T. (1987), *Tides, Surges and Mean-Sea Level: A Handbook for Engineers and Scientists*, 472 pp., John Wiley, Hoboken, N. J.

Sandstrom, H. (1980), On the wind-induced sea level changes on the Scotian shelf, *J. Geophys. Res.*, *85*, 461–468.

Stramma, L., and G. Siedler (1988), Seasonal changes in the North Atlantic subtropical gyre, *J. Geophys. Res.*, *93*, 8111–8118.

Tsimplis, M. N., and M. Rixen (2002), Sea level in the Mediterranean Sea: The contribution of temperature and salinity changes, *Geophys. Res. Lett.*, *29*(23), 2136, doi:10.1029/2002GL015870.

Tsimplis, M. N., and P. L. Woodworth (1994), The global distribution of the seasonal sea level cycle calculated from coastal tide gauge data, *J. Geophys. Res.*, *99*, 16,031–16,039.

Wooster, W. S., A. Bakun, and D. R. McLain (1976), The seasonal upwelling cycle along the eastern boundary of the North Atlantic, *J. Mar. Res.*, *34*, 131–141.

World Ocean Atlas 2001 [CD-ROM] (2001), http://www.nodc.noaa.gov/OC5/WOA01/pr_woa01.html, Natl. Oceanogr. Data Cent., Silver Spring, Md.

Wunsch, C. (1991), Large-scale response of the ocean to atmospheric forcing at low frequencies, *J. Geophys. Res.*, *96*, 15,083–15,092.

————————————

E. Alvarez Fanjul, Area del Medio Físico, Puertos del Estado, Av. Partenón, 10, E-28042 Madrid, Spain.

J. Delgado, J. Del Río, and J. García-Lafuente, Departamento de Física Aplicada II, Universidad de Málaga, E-29071 Málaga, Spain. (vanndu@teleline.es; jorge.delrio@ctima.uma.es; glafuente@ctima.uma.es)

D. Gomis, Institut Mediterrani d'Estudis Avançats, Miquel Marqués, 21, E-07190 Esporles, Mallorca, Spain.